J. Fluid Mech. (1983), *vol.* 133, *pp.* 413–425
Printed in Great Britain

The lift on an aerofoil in starting flow

By J. M. R. GRAHAM
Department of Aeronautics, Imperial College, London SW7 2BY

(Received 26 January 1983)

An analysis is given of the initial development of the lift on an aerofoil in inviscid starting flow. It is shown that because of the spiral shape of the vortex sheet shed initially from the trailing edge the lift and drag are both singular at the start of impulsive motion. This result is in contrast with the prediction of finite forces by methods that assume the vortex sheet to be initially planar. The effect of a steady rate of change of incidence following the sudden onset of transverse (heaving) motion of an aerofoil in a steady stream is also discussed.

1. Introduction

Chow & Huang (1982) have derived results in a recent paper for the initial development of lift and drag on an impulsively started aerofoil in inviscid incompressible flow. In particular they studied the effect of the trailing-edge angle τ, showing that the lift

$$L(t) \propto t^{(2-\kappa)/(\kappa-1)},$$

where $\kappa = 2-\tau/\pi$ and the time t is measured from the start of the impulsive motion. This result predicts a zero value of lift for all aerofoils at $t = 0$, the value being non-zero only if the trailing edge is a cusp ($\tau = 0$). The analysis leading to this result satisfies the exact normal-velocity boundary condition of inviscid flow on the surface of the aerofoil profile, but assumes that, for small enough times, the vortex sheet shed at the trailing edge can be approximated by a short *planar* element, coplanar with the higher velocity surface at the trailing edge of the aerofoil (figure 1). However, this assumption, although frequently used and found to give an adequate representation of the latest piece of an extensive sheet shed from the trailing edge, is not generally a satisfactory representation of the *whole* sheet, however small.

The development of a vortex sheet shed from a sharp edge under a variety of inviscid starting flows has been calculated by Pullin (1978). In all the cases that he considered, including the impulsive start, the vortex sheet was found to roll up as a self-similar spiral above the lee-side of the edge. The sheet cannot therefore be represented accurately by a plane element at *any* time after an impulsive start, however short. In fact a spiral sheet is better approximated by a single concentrated point vortex in the neighbourhood of its centroid. It will be shown here that such a representation gives a time dependence for the lift in impulsively started flow,

$$L(t) \propto t^{(3-2\kappa)/(2\kappa-1)},$$

which is quite different from that obtained by making the planar sheet assumption. The lift given by the above expression has a weak singularity at $t = 0$ for all aerofoils with a trailing edge angle $\tau < \frac{1}{2}\pi$, i.e. for all practical aerofoils.

A concentrated-vortex method is used in this paper to calculate some quantitative values. This simplified model of a spiral vortex sheet was first proposed by Brown

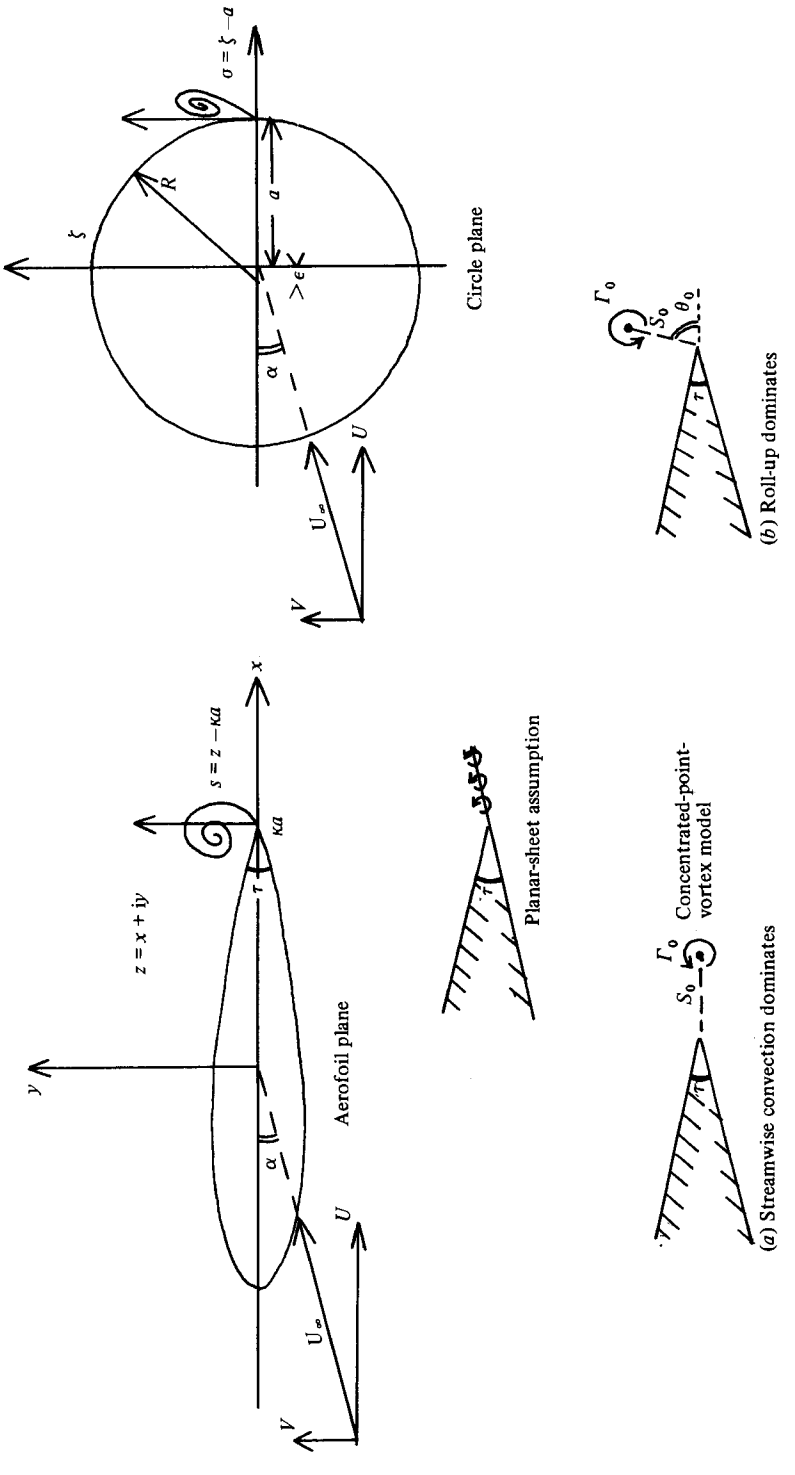

FIGURE 1. Aerofoil, vortex sheet and Kármán–Trefftz transformation.

& Michael (1955) for separated flow over slender wings and later extended by Rott (1956) to unsteady flows past isolated sharp edges. The more complete representation of the sheet used by Pullin could, of course, be used here also. However, comparisons with more accurate methods indicate that the concentrated-point-vortex model predicts overall quantities such as the circulation or lift to acceptable accuracy provided that the trailing-edge angles are not too large ($< \frac{1}{4}\pi$).

If, however, the aerofoil in a uniform stream starts to move so that its relative incidence to the stream changes continuously at a sufficiently gradual rate, then it will be shown that the rate of roll-up of the vortex sheet is much weaker. In this case the sheet is convected downstream faster than it rolls up and the time dependence of the lift is as given by the planar-sheet assumption. It may therefore be assumed that the planar sheet is a reasonable approximation for gradual changes of incidence in a continuously flowing stream.

2. Analysis

We consider inviscid flow past a Kármán–Trefftz aerofoil profile of chord c as an example. The transformation

$$\frac{z-\kappa a}{z+\kappa a} = \left(\frac{\zeta-a}{\zeta+a}\right)^{\kappa}$$

transforms the aerofoil shown in figure 1 with trailing-edge angle $\tau = \pi(2-\kappa)$ into a circle of radius $R = a+\epsilon$ in the ζ-plane. The displacement ϵ depends on the thickness-to-chord ratio of the aerofoil.

In the neighbourhood of the trailing edge at $z = \kappa a$ a local coordinate system is $s = z-\kappa a$ and correspondingly $\sigma = \zeta-a$. The local form of the transformation in terms of these is

$$\sigma = 2a\left\{\left(\frac{s}{2\kappa a}\right)^{1/\kappa} + \left(\frac{s}{2\kappa a}\right)^{2/\kappa} + \ldots\right\}.$$

A non-circulatory flow relative to the aerofoil has chordwise and transverse components $U(t)$ and $V(t)$. The corresponding complex potential in the ζ-plane is

$$W_{\infty}(\zeta) = U\left(\zeta+\epsilon+\frac{R^2}{\zeta+\epsilon}\right) - iV\left(\zeta+\epsilon-\frac{R^2}{\zeta+\epsilon}\right).$$

Near the trailing edge in the z-plane this becomes

$$W_{\infty}(s) = 2RU - 2\mathrm{i}V(2a)^{1-1/\kappa}\kappa^{-1/\kappa}s^{1/\kappa} + (U+\mathrm{i}V)(2a)^{2(1-1/\kappa)}\kappa^{-2/\kappa}R^{-1}s^{2/\kappa} + \ldots.$$

The spatially constant term $2RU$ has no effect on the velocity field or vortex shedding and may be ignored.

Following Pullin (1978), the equation for the development of the vortex sheet $s = \tilde{s}(\Gamma, t)$ shed from the trailing edge in response to the flow round it is

$$\frac{\partial \tilde{s}^*}{\partial t} = \left.\frac{\partial W}{\partial s}\right|_{s=\tilde{s}}, \tag{1}$$

where $*$ indicates a complex conjugate.

In addition a Kutta–Joukowski condition must be applied at the trailing edge:

$$\left.\frac{\partial W}{\partial \sigma}\right|_{s=0} = 0. \tag{2}$$

The complex potential $W = W_\infty + W_\Gamma$, where W_Γ is the part due to the vortex sheet. Replacing the interaction of the vortex sheet with the body by an image sheet in the circular profile in the transformed plane,

$$\frac{\partial W}{\partial s} = \frac{\partial W_\infty}{\partial s} + \frac{1}{2\pi \mathrm{i}} \frac{\partial \sigma}{\partial s} \left\{ \int_0^{\Gamma_0} \frac{\mathrm{d}\Gamma}{\sigma - \tilde{\sigma}(\Gamma, t)} + \int_0^{-\Gamma_0} \frac{\mathrm{d}\Gamma}{\sigma - \tilde{\sigma}_\mathrm{I}(\Gamma, t)} \right\}. \tag{3}$$

Γ is the circulation of the vortex sheet (total circulation Γ_0) from the origin to the point $\tilde{s}$ (or $\tilde{\sigma}$) on the sheet. $\tilde{\sigma}_\mathrm{I}$ is the image of $\tilde{\sigma}$ in the ζ-plane circle.

Hence the convection equation for the vortex sheet becomes

$$\begin{aligned} \frac{\partial \tilde{s}^*}{\partial t} = & -\frac{2\mathrm{i}}{\kappa^2} V(t) (2a\kappa)^{1-1/\kappa} \tilde{s}^{1/(\kappa-1)} + \frac{2U(t)}{\kappa^3 R} (2a\kappa)^{2(1-1/\kappa)} \tilde{s}^{2/(\kappa-1)} \\ & + \frac{2\mathrm{i}}{\kappa^3 R} V(t) (2a\kappa)^{2(1-1/\kappa)} \tilde{s}^{2/(\kappa-1)} \\ & + \frac{\tilde{s}^{1/\kappa-1}}{2\pi \mathrm{i} \kappa} \left\{ \int_0^{\Gamma_0} \frac{\mathrm{d}\Gamma}{\tilde{s}^{1/\kappa} - (\tilde{s}'(\Gamma))^{1/\kappa}} + \int_0^{-\Gamma_0} \frac{\mathrm{d}\Gamma}{\tilde{s}^{1/\kappa} - (\tilde{s}'_\mathrm{I}(\Gamma))^{1/\kappa}} \right\}, \end{aligned} \tag{4}$$

and the Kutta–Joukowski condition

$$\int_0^{\Gamma_0} \frac{\mathrm{d}\Gamma}{(\tilde{s}(\Gamma))^{1/\kappa}} + \int_0^{-\Gamma_0} \frac{\mathrm{d}\Gamma}{(\tilde{s}_I(\Gamma))^{1/\kappa}} = \frac{(2a\kappa)^{1-1/\kappa}}{4\pi\kappa} V(t). \tag{5}$$

We now consider the case of a starting flow given to leading order in t by

$$U = \hat{U} t^\beta + \ldots, \quad V = \hat{V} t^\gamma + \ldots.$$

Hence we may assume

$$\Gamma = \hat{\Gamma} t^\mu + \ldots, \quad \tilde{s} = \hat{s} t^\nu + \ldots,$$

where ν is expected to be positive since the sheet grows continuously with time, and $\hat{s}$ and $\hat{\Gamma}$ are the similarity variables describing the shape of the vortex sheet and its strength to lowest order in the time.

Substituting in (5),

$$\mu - \frac{\nu}{\kappa} = \gamma.$$

Using this result in (4) gives five terms from left to right depending on t to the following powers:

$$\nu - 1, \quad \gamma + \frac{\nu}{\kappa} - \nu, \quad \beta + \frac{2\nu}{\kappa} - \nu, \quad \gamma + \frac{2\nu}{\kappa} - \nu, \quad \gamma + \frac{\nu}{\kappa} - \nu.$$

Since $\nu \geqslant 0$, the fourth term clearly never influences the leading-order time development of the sheet. There are therefore two possibilities:

(*a*) $\beta + \frac{2\nu}{\kappa} - \nu < \gamma + \frac{\nu}{\kappa} - \nu,$

so that the U-velocity dominates the development of the vortex sheet; in this case

$$\nu = \frac{\beta + 1}{2 - 2/\kappa}; \tag{6}$$

(*b*) $\gamma + \frac{\nu}{\kappa} - \nu < \beta + \frac{2\nu}{\kappa} - \nu,$

in which case the V-velocity round the edge is dominant and

$$\nu = \frac{\gamma + 1}{2 - 1/\kappa}. \tag{7}$$

Both these alternatives lead to $\nu > 0$, thus justifying the *a priori* assumption. It will be shown that the first alternative leads to the centroid of the shed vorticity moving approximately in the direction of the bisector of the trailing-edge angle. It is therefore closer to the representation of the sheet by a short plane element as suggested by Chow & Huang. However, this alternative only applies if

$$\beta \leqslant (\gamma+1)\left(\frac{2\kappa-2}{2\kappa-1}\right)-1. \tag{8}$$

In a starting flow past an aerofoil at fixed incidence α,

$$U = U_\infty(t)\cos\alpha, \quad V = U_\infty(t)\sin\alpha, \quad \beta = \gamma.$$

Hence (8) is never satisfied since $(2\kappa-2)/(2\kappa-1) < 1$ for all edge angles. But if the vortex shedding and build-up of circulation is more gradual, as for example when an aerofoil starts to change its effective incidence at a moderate rate in a uniformly flowing stream,

$$\beta = 0,$$

and provided that

$$\gamma > \frac{\frac{1}{2}\pi}{\pi-\tau},$$

the U-velocity dominates and the first alternative does apply. In this case convection of the sheet downstream is more significant than the rate of roll-up, and the plane sheet is likely to be a good approximation.

In order to demonstrate the importance of the initial shape of the vortex sheet on the development of lift on the aerofoil, we now calculate some examples using the concentrated-point-vortex representation of the sheet.

2.1. *Concentrated-point-vortex representation* (*figure* 1)

In this simplified model of a spiral vortex sheet, the sheet is replaced by a concentrated point vortex Γ_0 at s_0 at the approximate 'centre' of the spiral joined to the trailing edge ($s = 0$) by a 'cut' in the plane across which the velocity potential is discontinuous. The cut represents the effect of the sheet feeding vorticity from the edge to the growing vortex core. The equations governing the growth and motion of the vortex have been derived by Rott (1956) and Graham (1977) for unsteady separated flow based on the original theory of Brown & Michael (1955) for steady separated flow over a slender wing.

They are a zero total force (complex) equation

$$\frac{\partial s_0^*}{\partial t}+\frac{s_0^*}{\Gamma_0}\frac{\partial \Gamma_0}{\partial t} = \left.\frac{\partial W}{\partial s}\right|_{s=s_0} \tag{9}$$

and the Kutta–Joukowski condition at the edge

$$\left.\frac{\partial W}{\partial \sigma}\right|_{\sigma=0} = 0, \tag{10}$$

$$\left.\frac{\partial W}{\partial s}\right|_{s=s_0} = \lim_{s\to s_0}\left[\frac{\partial \sigma}{\partial s}\frac{\partial W}{\partial \sigma}-\frac{\mathrm{i}\Gamma_0}{2\pi(s-s_0)}\right],$$

$$\frac{\partial W}{\partial \sigma} = \frac{\partial W_\infty}{\partial \sigma}+\frac{\mathrm{i}\Gamma_0}{2\pi(\sigma-\sigma_0)}-\frac{\mathrm{i}\Gamma}{2\pi(\sigma-\sigma_{I0})}, \tag{11}$$

where $\sigma_{I0} = -R\sigma_0^*/(R+\sigma_0^*)$ is the image of σ_0 in the circle, for small σ_0/R. Equations

(9)–(11) are dimensionally exactly the same as equations (1)–(3) for the continuous sheet that they replace. Therefore if, as before,

$$\Gamma_0 = \hat{\Gamma} t^{\mu} + \ldots, \quad s_0 = \hat{s} t^{\nu} + \ldots,$$

then either

$$\nu = \frac{\beta+1}{2-2/\kappa} \quad \text{if } U \text{ dominates,}$$

or

$$\nu = \frac{\gamma+1}{2-1/\kappa} \quad \text{if } V \text{ dominates,}$$

and

$$\mu = \frac{\nu}{\kappa+\gamma}.$$

2.2. *Aerofoil starting flows*

We consider a starting flow $U_\infty(t) = \hat{U}_\infty t^{\beta}$ at incidence α past the aerofoil. Thus

$$U = \hat{U}_\infty \cos\alpha t^{\beta}, \quad V = \hat{U}_\infty \sin\alpha t^{\beta}, \quad \gamma = \beta.$$

In this case it is clear that the second alternative (V dominant) applies for all values of β and all trailing-edge angles.

Substituting in (9)–(11) (see Graham 1977) gives without further approximation

$$\Gamma_0 = -8\pi\kappa^{-\frac{1}{2}}\chi_v\left(\frac{\hat{U}_\infty t^{\beta+1}\sin\alpha}{a}\right)^{2\kappa/(2\kappa-1)} a^2 t^{-1}, \tag{12}$$

$$s_0 = 2\kappa\chi_{\mathrm{v}}^{\kappa}\left(\frac{\hat{U}_\infty t^{\beta+1}\sin\alpha}{a}\right)^{\kappa/(2\kappa-1)} a\,\mathrm{e}^{\mathrm{i}\theta_0}, \tag{13}$$

where

$$\theta_0 = -\kappa\cos^{-1}(\tfrac{1}{2}\kappa^{\frac{1}{2}}),$$

$$\chi_{\mathrm{v}} = \left[\frac{(4-\kappa)^{\frac{1}{2}}(\kappa-1)(2\kappa-1)}{2\kappa^4(3\beta\kappa+\kappa+1)}\right]^{1/(2\kappa-1)}.$$

The form of these two equations can also be obtained very simply by considering a local lengthscale $\mathscr{L}$ for the flow near the edge. Therefore from dimensional considerations and its dependence on s, the local potential

$$W_\infty(s) \propto \mathscr{L}^{2-1/\kappa} s^{1/\kappa} t^{-1},$$

where

$$\mathscr{L} \propto [Vta^{1-1/\kappa}]^{\kappa/(2\kappa-1)}$$

from the original form of W_∞.

If $s_0 \propto \mathscr{L}$ and $\Gamma_0 \propto \mathscr{L}^2 t^{-1}$ the time dependence of (12) and (13) follows.

The expression for θ_0 shows that the vortex core leaves the trailing edge at a large angle to the stream (assuming a typical magnitude for α). For example in the case of a cusped trailing edge ($\tau = 0, \kappa = 2$) the vortex moves in a perpendicular direction to that of the cusp and the vortex forms *above* the trailing edge (figure 2). This initial direction of movement of the vortex, which is in agreement with Pullin's (1978) more detailed calculations, is responsible for the large initial rate of vortex shedding

$$\frac{\partial\Gamma_0}{\partial t} \sim t^{2(1-\kappa)/(2\kappa-1)}$$

and hence the comparatively large initial force on the aerofoil. Direct comparison of

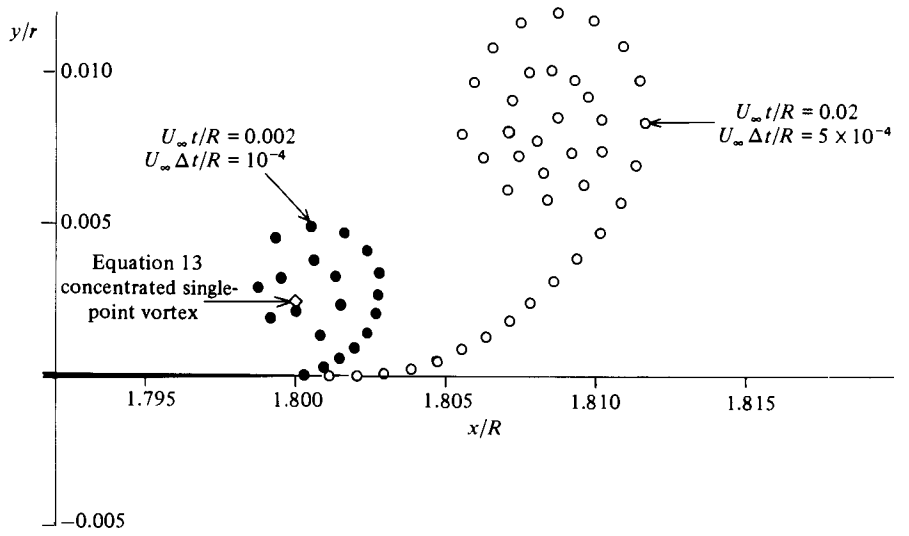

FIGURE 2. Initial vortex sheet development for 13% thick Joukowski aerofoil in impulsively started flow at 10° incidence. Aerofoil chord = $3.6364R$.

(12) with Pullin's result from an isolated edge in the case of unit impulsive starting flow ($\beta = 0$, $U_\infty \sin\alpha/a = 1$) round a cusp ($\tau = 0$) gives:

$$\Gamma_0 = -2.493t^{\frac{1}{3}} \text{ (equation (12))},$$
$$\Gamma_0 = -2.398t^{\frac{1}{3}} \text{ (Pullin)}.$$

This gives an indication of the magnitude of the error in the circulation predicted by the concentrated vortex method. It should, however, be emphasized that detailed quantities such as pressure distributions are predicted much less accurately.

The complex force Z per unit span of the aerofoil can be most conveniently evaluated by momentum considerations from a form of Blasius theorem:

$$Z = -\mathrm{i}\rho \frac{\partial}{\partial t} \oint_\infty W \,\mathrm{d}z,$$

where the integral is taken round a circuit at infinity surrounding the whole vortex wake including the starting vortex and the aerofoil. This is the unsteady analogue of an integral for the force on a slender body in terms of its crossflow potential (Brown & Michael 1955) and can be shown to be equivalent to the usual form of Blasius' theorem (Graham 1980).

Substituting for W and evaluating the integral by the residue theorem:

$$Z = 2\pi\rho \frac{\partial U_\infty}{\partial t}\{\mathrm{e}^{\mathrm{i}\alpha}R^2 - \tfrac{1}{2}\mathrm{e}^{-\mathrm{i}\alpha}\kappa(\kappa-1)a^2\} - \frac{2a\mathrm{i}\rho}{(2a\kappa)^{1/\kappa}} \frac{\partial}{\partial t}\{\Gamma_0(s_0^{1/\kappa} + s_0^{*1/\kappa})\}$$
$$= 2\pi\rho \frac{\partial U_\infty}{\partial t}\{\mathrm{e}^{\mathrm{i}\alpha}R^2 - \tfrac{1}{2}\mathrm{e}^{-\mathrm{i}\alpha}\kappa(\kappa-1)a^2\} + \frac{16(2+\beta(2\kappa+1))\pi\mathrm{i}\rho}{2\kappa-1}\chi_{\mathrm{v}}^2$$
$$\times \left(\frac{U_\infty t^{\beta+1}\sin\alpha}{a}\right)^{(3-2\kappa)/(2\kappa-1)} a\hat{U}_\infty^2 t^{2\beta}\sin^2\alpha. \tag{14}$$

The first term of this expression is the inertia force arising from acceleration of the non-circulatory (attached) flow over the profile and the second term is the contribution

from the circulation. The second term is independent of whether the flow is accelerating and the aerofoil stationary, as implicitly assumed here, or whether the aerofoil is accelerating in otherwise stationary fluid, the more practical case. In the latter case the first term is reduced by the so-called Froude–Krylov force $\rho(\partial U_\infty/\partial t)\,A$. This force represents the added contribution of the undisturbed pressure gradient in the fluid acting as a buoyancy force on the volume A per unit length of the profile.

2.3. *Impulsively started motion* ($\beta = 0$)

In this case the inertia force is zero for all $t > 0$. (It has an infinite value at $t = 0$.) Henceforth for $t > 0$ both moving aerofoil and moving fluid situations are dynamically the same. U_∞ = constant for $t > 0$, therefore

$$Z \sim t^{(3-2\kappa)/(2\kappa-1)} \quad \text{in equation (14).}$$

Hence Z is singular as $t \to 0$ for all $\kappa > \frac{3}{2}$, i.e. for all aerofoils with trailing-edge angles $\tau < \frac{1}{2}\pi$. This result contrasts with the finite ($\tau = 0$) or zero limits obtained by Chow & Huang (1982) for Z as $t \to 0$ assuming the vortex sheet to be initially plane.

Taking the lift force $L(t)$ as the component of Z perpendicular to the free stream and using the result for the steady flow lift on the aerofoil

$$\bar{L} = 4\pi\rho U_\infty^2\, R \sin\alpha,$$

the initial ratio of the lift coefficients is

$$\frac{C_L(t)}{C_{\bar{L}}} = \left\{\frac{\beta}{4}\kappa(\kappa-1)\left(\frac{\hat{U}_\infty t^{\beta+1}\sin\alpha}{a}\right)^{-1} + \frac{2(2+\beta(2\kappa+1))}{2\kappa-1}\chi_v^2 \times\left(\frac{\hat{U}_\infty t^{\beta+1}\sin\alpha}{a}\right)^{(3-2\kappa)/(2\kappa-1)}\right\}\frac{a}{R}\sin 2\alpha \quad (15)$$

for general starting flows, and

$$\frac{C_L(t)}{C_{\bar{L}}} = \frac{8\chi_v^2\cos\alpha}{2\kappa-1}\left(\frac{a}{R}\right)^2\left(\frac{R\sin\alpha}{a}\right)^{2/(2\kappa-1)}\left(\frac{U_\infty t}{R}\right)^{(3-2\kappa)/(2\kappa-1)} \quad (16)$$

in terms of $U_\infty t/R$ for impulsively started flow. Equation (16) is compared with the results of Chow & Huang's plane-sheet assumption in table 1 for two trailing-edge angles and two incidences. Direct comparison is only possible if the aerofoil's thickness/chord ratio is also specified since the dependence on the ratio R/a is different in the two cases. However, for thin aerofoils $(R/a)^{2/(2\kappa-1)}$ is close to unity so qualitative comparison is possible. The streamwise component of (14) shows similarly that the drag force is singular at $t = 0$.

The most important effect of the present theory is to show that the lift *decreases* initially in the case of an impulsive start before reaching a minimum and then increasing in the usual monotonic way thereafter. Apparently no numerical computations have revealed this behaviour previously. There are two probable reasons for this: the minimum lift is reached in a very short time by normal computational standards, $U_\infty t/c = O(10^{-1})$, and the first time step of a computation necessarily represents a finite rather than infinite acceleration to the final velocity. Most numerical calculations, such as those of Giesing (1968) and Basu & Hancock (1978) represent the vortex sheet by discrete points or elements which are shed in the downstream sector formed by the extension of the aerofoil upper and lower surfaces at the trailing edge. In fact, as Basu & Hancock show, such a method can be made to take up naturally the correct orientation for tangential separation once the sheet has started to develop.

τ	$U_\infty t/R$	$\frac{C_L}{C_{\bar{L}}}\left(\frac{a}{R}\right)^{-\frac{4}{3}}$ $\alpha = 1°$	$\alpha = 10°$	$\frac{C_L}{C_{\bar{L}}}\left(\frac{a}{R}\right)^{-2}$ Chow & Huang (1982) (small α)
0	10^{-6}	2.242	10.217	0.5 (independent of t)
	10^{-5}	1.041	4.742	
	10^{-4}	0.483	2.201	
	10^{-3}	0.224	1.022	
	10^{-2}	0.104	0.474	
	10^{-1}	0.048	0.220	
		$\frac{C_{\bar{L}}}{C_L}\left(\frac{a}{R}\right)^{-1.286}$		$\frac{C_L}{C_{\bar{L}}}\left(\frac{a}{R}\right)^{-2}$
	$U_\infty t/R$	$\alpha = 1°$	$\alpha = 10°$	Chow & Huang (1982) (small α)
0.1π	10^{-6}	0.943	4.792	0.134
	10^{-5}	0.488	2.482	0.168
	10^{-4}	0.253	1.286	0.212
	10^{-3}	0.131	0.666	0.267
	10^{-2}	0.068	0.345	0.336
	10^{-1}	0.035	0.179	0.423

TABLE 1

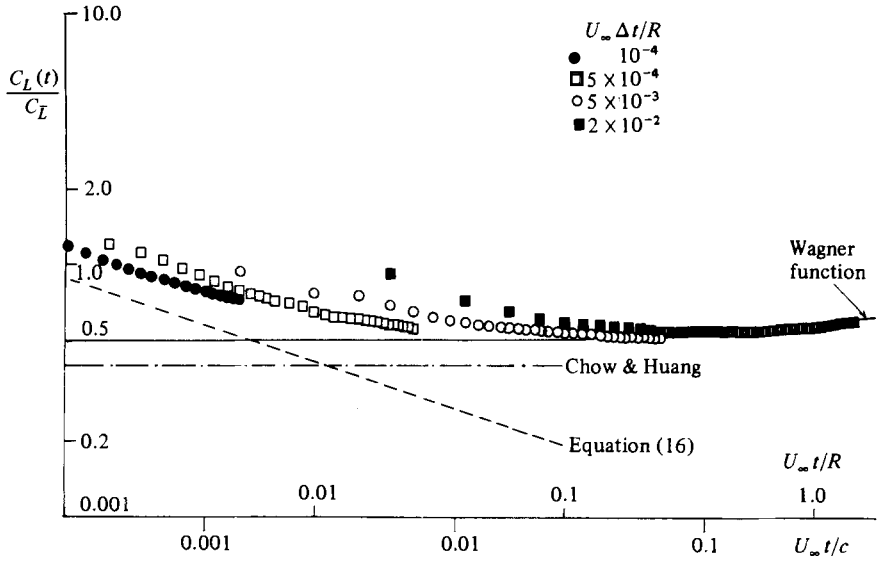

FIGURE 3. Lift coefficient for impulsively started flow as figure 2: —, Wagner function; – – –, equation (16); –·–·–, Chow & Huang (1982).

In order to demonstrate the reality of the asymptotic result obtained above for small times, a numerical computation of the sheet development for an aerofoil in impulsive flow has been carried out using the discrete (multi)vortex method. In order not to bias the method towards the type of roll-up anticipated, all the vortices were shed sequentially tangentially from the trailing edge. Roll-up of the vortex sheet was allowed to occur haphazardly without representation of the inner part of the spiral

by a core vortex to promote stability. For this reason the structure of the inner part of the vortex spiral is destroyed by the rapid growth of short-wavelength instabilities discussed by Moore (1974). The aerofoil was a Joukowski profile (i.e. one of the Karman–Trefftz family with $\tau = 0$) with $\epsilon/R = 0.1$, giving a thickness/chord ratio of 13%. Computations were carried out with the aerofoil at 10° incidence to the flow using very small time steps $U_\infty \Delta t/R$ of order 10^{-4} and above. The initial development of the predicted sheet, which is subject to stronger roll-up than downstream convection, takes place above the rear part of the aerofoil's upper surface (figure 2). This result is in agreement with the concentrated point vortex result, as is the prediction for the lift coefficient shown in figure 3. The magnitude of the initial peak in the lift coefficient is clearly dependent on the size of time step Δt used. This suggests that in the limit $\Delta t \to 0$ the $t^{-\frac{1}{2}}$ singular behaviour would be recovered and explains why no peak may be predicted in 'normal' computations, which use a time step $U_\infty \Delta t/R$ of order 10^{-1} or larger. These figures also show how, as time elapses, effects of streamwise convection become increasingly significant, the rolled-up vortex is swept downstream and the well-established rising C_L curve is reached.

Real starting flows can never be truly impulsive and must have finite acceleration. 'Impulsively' started motion consists of a large but finite initial acceleration with $\hat{U}_\infty$ large and $\beta > 1$. Inertia therefore dominates the force at $t = 0$ and no singularity occurs. However, the results of the multivortex calculations shown in figure 3 similarly represent flows with large but effectively finite acceleration during the first time step. These results show that increasing the initial acceleration increases the initial peak in the lift due to circulation at the end of the acceleration phase in addition to the larger but more transitory inertia force, which occurs during the acceleration phase only. If, however, the initial acceleration takes place over a non-dimensional time $U_\infty t/c$ greater than about 10^{-1}, the initial peak in the circulatory part of the lift will disappear, while the inertia force will remain.

2.4. *Cases when the chordwise velocity dominates the initial development*

If

$$\beta < (\gamma+1)\left(\frac{2\kappa-2}{2\kappa-1}\right)-1$$

then the leading-order solution to (9)–(11) is

$$\Gamma_0 = 4\pi\kappa^{-1/(\kappa-1)}\chi_{\mathrm{u}}\left(\frac{Ut}{R}\right)^{1/2(\kappa-1)}\left(\frac{Vt}{a}\right)a^2t^{-1},$$

$$s_0 = 2\kappa^{-1/(\kappa-1)}\chi_{\mathrm{u}}^{\kappa}\left(\frac{Ut}{R}\right)^{\kappa/2(\kappa-1)}a,$$

where

$$\chi_{\mathrm{u}} = \left[\frac{4(\kappa-1)}{\kappa(2\gamma(\kappa-1)+(\beta+1)(\kappa+1)}\right]^{1/2(\kappa-1)}.$$

s_0 is predicted to be real by this result, and therefore the model predicts that the centroid of vorticity should move initially along the line bisecting the trailing-edge angle. The transverse velocity field and roll-up of the vortex sheet are relatively weaker, and streamwise convection dominates the development of the sheet.

In this case the circulatory part of the force on the aerofoil is given by

$$Z_\Gamma = 16\pi\mathrm{i}\left(\gamma+\frac{\beta+1}{\kappa-1}\right)\kappa^{-2/(\kappa-1)}\chi_{\mathrm{u}}^2\left(\frac{Ut}{R}\right)^{1/(\kappa-1)}\left(\frac{Vt}{a}\right)^{-1}\rho V^2 a. \tag{17}$$

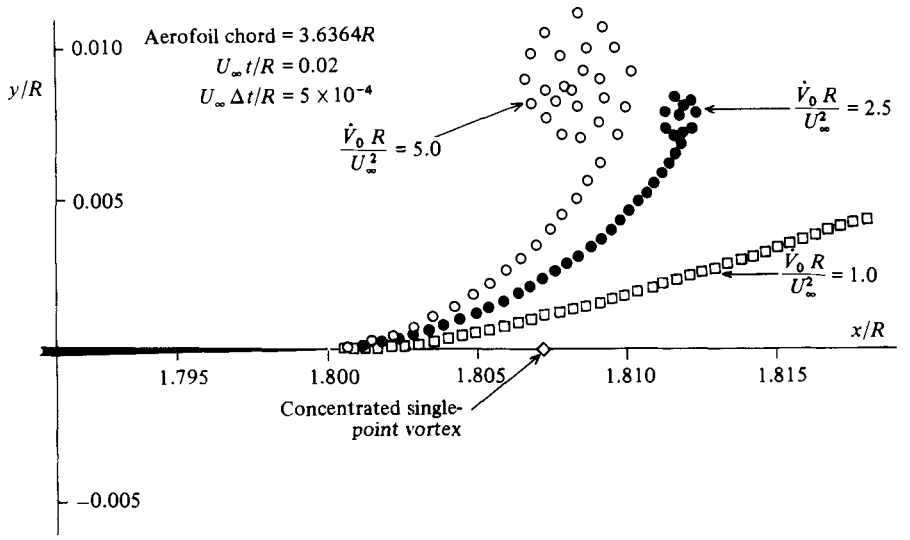

FIGURE 4. Initial vortex-sheet development for aerofoil in heaving motion.

This formula (17), if adopted, incorrectly, for the case of impulsively started flow, gives

$$Z_\Gamma \sim t^{(2-\kappa)/(\kappa-1)},$$

which is the time dependence derived by Chow & Huang for the lift force. The singular behaviour of the previous solution (15) at $t = 0$ is absent. However, a type of flow in which U dominates and (17) gives the correct dependence on the time for the initial development of the force on an aerofoil occurs when an aerofoil in a steady stream suddenly starts to change its effective incidence at a constant rate. For example, in the case when the aerofoil suddenly starts to move transversely with constant acceleration $\dot{V}_0$,

$$U = U_\infty, \quad \text{i.e.} \quad \beta = 0,$$
$$V = \dot{V}_0 t, \quad \text{i.e.} \quad \gamma = 1.$$

Therefore, from (17), including the inertia force,

$$\frac{C_L(t)}{C_{\bar{L}}} = \frac{1}{2}\left(1 + \frac{\kappa(\kappa-1)a^2}{2R^2} - \frac{A}{2\pi R^2}\right) + \frac{4}{\kappa-1}\kappa^{(\kappa-3)/(\kappa-1)}\frac{\chi_u^2 a^2}{R^2}\left(\frac{U_\infty t}{R}\right)^{1/(\kappa-1)}. \tag{18}$$

$C_{\bar{L}}$ is here a representative steady lift coefficient $8\pi R^2 \dot{V}_0/U_\infty^2 c$ (when the aerofoil is at incidence arcsin $(\dot{V}_0 R/U_\infty^2)$) and A is the cross-sectional area of the aerofoil. The inertia (first) term of the lift force in (18) dominates the circulatory contribution to the lift at small times.

Figure 4 shows the vortex sheet shed from a Joukowski aerofoil undergoing transverse motion in a steady stream, computed by a discrete vortex method with very small time steps. Comparison with figure 2 for impulsively started flow shows the dominance of streamwise convection over roll-up of the vortex sheet. Indeed, it appears that for sufficiently small values of transverse acceleration the discrete vortex method predicts the shedding of an unrolled-up sheet for a large number of time steps. The time history of the circulatory part of the lift force obtained by this method shows a nearly linear growth with time close to that predicted by (18) (figure 5). The initially faster rate of growth is due to the effect of the finite initial time step.

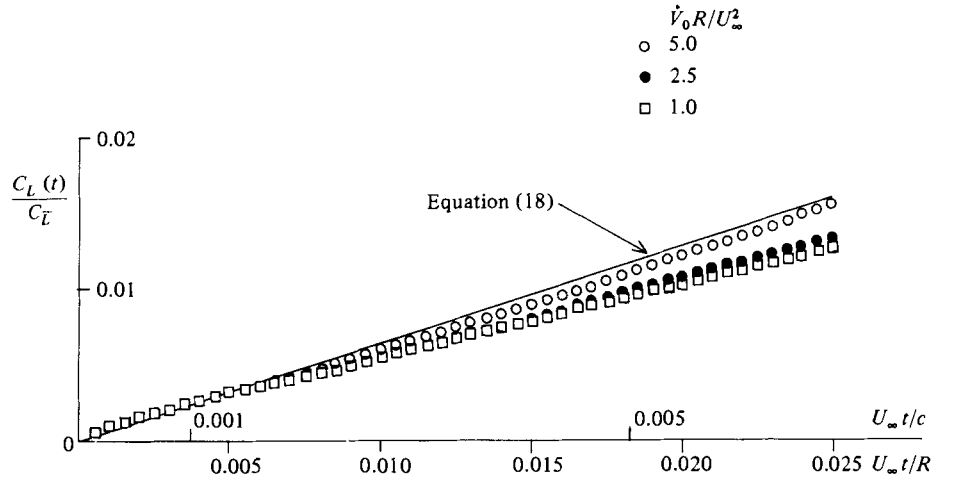

FIGURE 5. Lift coefficient (circulatory part) for aerofoil in heaving motion. ——, equation (18) circulatory part.

2.5. *Higher-order terms*

If we substitute

$$\Gamma_0 = \hat{\Gamma}_1 t^{\mu_1} + \hat{\Gamma}_2 t^{\mu_2} + \ldots \quad (\mu_2 > \mu_1),$$
$$s_0 = \hat{s}_1 t^{\nu_1} + \hat{s}_2 t^{\nu_2} + \ldots \quad (\nu_2 > \nu_1)$$

in (9)–(11) and consider the case when V dominates, we obtain

$$\mu_1 = \frac{1}{2\kappa - 1}, \quad \nu_1 = \frac{\kappa}{2\kappa - 1}$$

as before, and in addition

$$\mu_2 = \frac{2}{2\kappa - 1}, \quad \nu_2 = \frac{\kappa + 1}{2\kappa - 1}.$$

Hence the circulatory part of the lift coefficient for an impulsive start

$$C_L \sim C_{L_1} t^{(3-2\kappa)/(2\kappa-1)} + C_{L_2} t^{(3-2\kappa+1/\kappa)/(2\kappa-1)} + C_{L_3} t^{(4-2\kappa)/(2\kappa-1)} + \ldots$$

When the trailing edge is a cusp, for example,

$$C_L \sim C_{L_1} t^{-\frac{1}{3}} + C_{L_2} t^{-\frac{1}{6}} + C_{L_3} t^0 + \ldots.$$

Thus the difference in order of magnitude of succeeding terms is small, and higher-order terms can be expected to have a significant influence unless t is very small indeed.

2.6. *Effects of viscosity and compressibility*

In a real viscous fluid, shedding of a vortex sheet at the trailing edge results from separation of a growing boundary layer. The thickness δ of the boundary layer on the aerofoil grows initially in a starting flow proportionally to $(\nu t)^{\frac{1}{2}}$, where ν is the kinematic viscosity. However, the scale of the shed vortex, for example, for an impulsive start, is given by

$$s_0 \sim (U_\infty t)^{\kappa/(2\kappa-1)} c^{(\kappa-1)/(2\kappa-1)}.$$

Hence the scale of the vortex will overtake that of the boundary-layer thickness in a time

$$t_{\mathrm{v}} \sim U_{\infty}^{-1} c R_{\mathrm{e}}^{1-2\kappa},$$

where R_{e} is the chord Reynolds number. For small or moderate trailing-edge angles ($\kappa \approx 2$) and practical Reynolds numbers this is a very small time, much smaller than those considered in the above inviscid analysis.

On the other hand, effects of compressibility, which should be expected to retard the initial growth of circulation, are significant over times smaller than

$$t_{\mathrm{c}} \sim a_{\infty}^{-1} c,$$

where a_{∞} is the speed of sound in the fluid. Thus compressibility effects are likely to be significant unless the Mach number is very small ($< 10^{-1}$).

3. Conclusions

It has been shown that the initial development of the lift on an aerofoil in inviscid incompressible starting or suddenly changed motion depends strongly on the rate at which the effective incidence changes compared with the rate of change, if any, of streamwise velocity, as well as the trailing-edge angle. In the case of starting flows, the shed vortex sheet rolls up initially *above* the trailing edge, and planar-sheet models are not appropriate for small times. In particular, impulsively started aerofoils with trailing-edge angles less than $\frac{1}{2}\pi$ are subject to an initial singularity in the lift followed by *decreasing* lift before the usually assumed monotonically increasing lift curve is reached.

REFERENCES

Basu, B. C. & Hancock, G. J. 1978 The unsteady motion of a two-dimensional aerofoil in incompressible inviscid flow. *J. Fluid Mech.* **87**, 159.

Brown, C. E. & Michael, W. H. 1955 On slender delta wings with leading edge separation. *NACA Tech. Note* 3430.

Chow, C.-Y. & Huang, M.-K. 1982 The initial lift and drag of an impulsively started aerofoil of finite thickness. *J. Fluid Mech.* **118**, 393.

Giesing, J. P. 1968 Non-linear two-dimensional unsteady potential flow with lift. *J. Aircraft* **5**, 135.

Graham, J. M. R. 1977 Vortex shedding from sharp edges. *Imperial College Aero. Rep.* 77-06.

Graham, J. M. R. 1980 The forces on sharp-edged cylinders in oscillatory flow at low Keulegan–Carpenter numbers. *J. Fluid Mech.* **97**, 331.

Moore, D. W. 1974 A numerical study of the roll-up of a finite vortex sheet. *J. Fluid Mech.* **63**, 225.

Pullin, D. I. 1978 The large-scale structure of unsteady self-similar rolled-up vortex sheets. *J. Fluid Mech.* **88**, p. 401.

Rott, N. 1956 Diffraction of a weak shock with vortex generation. *J. Fluid Mech.* **1**, 111.